Using a Soil Hydrology Model to Obtain Regionally Averaged Soil Moisture Values

TODD M. CRAWFORD AND DAVID J. STENSRUD

NOAA/National Severe Storms Laboratory, Norman, Oklahoma

TOBY N. CARLSON

The Pennsylvania State University, University Park, Pennsylvania

WILLIAM J. CAPEHART

South Dakota School of Mines and Technology, Rapid City, South Dakota

(Manuscript received 10 August 1999, in final form 22 April 2000)

ABSTRACT

The Soil Hydrology Model (SHM) was modified, and daily simulations of soil volumetric water content were made at 38 Oklahoma Mesonet sites for July 1997. These model results were compared with soil moisture observations made at the mesonet sites at depths of 5, 25, 60, and 75 cm. This work is believed to be the first time that a hydrological model has been evaluated with in situ soil moisture measurements over such an extensive area spanning several climate zones.

Comparisons of time series between the observed and modeled domain-averaged volumetric water content at 5 cm revealed similar phase and amplitude changes, a coefficient of determination (R^2) of 0.64, and small mean bias and root-mean-square errors (MBE and rmse) of 0.03 and 0.09, respectively. At 25, 60, and 75 cm, the model performance was slightly worse, with R^2 values between 0.27 and 0.40, MBE between -0.01 and 0.02, and rmse between 0.11 and 0.13. The model response to changes in soil water at these levels was sluggish, possibly because of, among other things, a lack of ability to model preferential downward water flow through cracks in the soil.

The results of this study suggest that SHM can be used effectively to initialize 5-cm soil moisture values in numerical prediction models. At deeper soil levels, however, the relatively small R^2 values and negligible MBE suggest that the model may be better suited for initializing a regionally averaged soil moisture value rather than unique gridbox values. These results illustrate the difficulty in using point measurements to validate a hydrological model, especially deeper in the soil where moisture values are more dependent on soil properties (which can vary sharply over small distances) and are less dependent on recent rainfall.

1. Introduction

Land surface schemes have been incorporated into meteorological models with spatial resolutions ranging from a few to hundreds of kilometers. Proper estimation of surface energy fluxes is extremely important in modeling both the planetary boundary layer and the planetary climate. Most of these schemes are very sensitive to surface characteristics such as vegetation type and coverage and soil type. Soil moisture also plays an important role in modulating boundary layer characteristics. Because there are few soil moisture observations available, however, parameterization of this quantity is difficult. Soil moisture often is estimated using an antecedent precipitation index (API; Wetzel and Chang 1988), which relates recent rainfall to estimated near-surface groundwater.

Current numerical weather prediction models are relatively crude in their parameterizations of soil moisture. The National Meteorological Center (now the National Centers for Environmental Prediction) Eta Model (Black 1994) uses the previous value of model-predicted soil moisture to initialize the latest run. The Fifth-Generation Pennsylvania State University–National Center for Atmospheric Research Mesoscale Model (Dudhia 1993) specifies a soil type and a climatological moisture availability value to initialize the model. Storm water runoff models also typically use an API-based scheme to initialize soil moisture (Vieux and Gaver 1994; Pereira Fo. and Crawford 1999).

Hydrological models describing the soil water profile have been developed recently (Groves 1989; Mahfouf 1991; Capehart and Carlson 1994) that potentially allow

Corresponding author address: Todd M. Crawford, Cooperative Institute for Mesoscale Meteorological Studies, National Severe Storms Laboratory, 1313 Halley Circle, Norman, OK 73069.
E-mail: crawford@nssl.noaa.gov

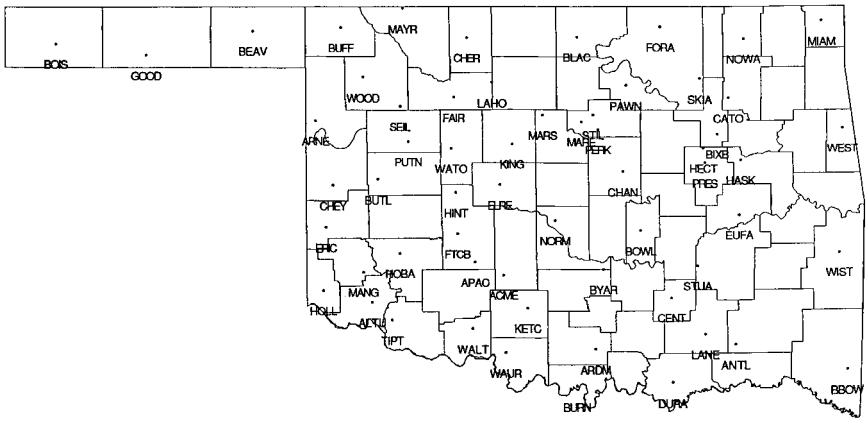

FIG. 1. The 60 stations of the Oklahoma Mesonet that measure soil moisture.

for a more precise specification of the magnitude of soil water at a given location. A logical next step in operational numerical prediction is to couple one of these hydrological models to a preexisting meteorological or storm runoff model to initialize the soil moisture more accurately.

Smith et al. (1994) stressed the need for a more physically realistic soil moisture initialization and used the Soil Hydrology Model (SHM; Capehart and Carlson 1994; 1997) to perform this task. At that time, however, there were limited soil moisture observations available to verify the SHM output. Liang et al. (1996) compared 1 yr of weekly soil moisture measurements representing the top 10, 50, and 100 cm to the three-layer Variable Infiltration Capacity (VIC; Liang et al. 1994) hydrological model, with promising results. Similarly, Cherkauer and Lettenmaier (1999) used measurements (in 0–10- and 10–100-cm layers) from two consecutive winter seasons to verify the VIC model. In both studies, however, point measurements from only one location were used.

In this study, SHM was run with a vertical resolution of 5 cm to a depth of 1 m. The unique, high-resolution soil moisture observations from the Oklahoma Mesonetwork (''Mesonet''; Brock et al. 1995) were used to evaluate SHM at 5, 25, 60, and 75 cm. These observations, at a horizontal resolution of approximately 50 km, span several climate zones, soil types, and vegetation types. This work is, we believe, the first time that such a high-resolution, spatially extensive dataset has been used to test a hydrological model.

The datasets used in this work will be described in section 2, followed by a more detailed description of SHM in section 3. Section 4 details comparisons between model output and observations, and the conclusions follow in section 5.

2. Data

Campbell Scientific, Inc., (CSI) 229-L heat dissipation matric potential sensors have been installed at 60 of the Mesonet sites (Fig. 1) at depths of 5, 25, 60, and 75 cm below the ground. These sensors are composed of a thermocouple and a heater wire enclosed in a hypodermic needle (Fig. 2). The needle is embedded in a cylindrical ceramic shield, whose porosity allows for equilibration with the surrounding soil (Reece 1996). An electric current is passed through the heater wire for 20 s, resulting in the production of heat from the resistance of the wire. This heat production is quantified as a rise in temperature within the sensor, as detected by the thermocouple. This temperature change ΔT can be related to the matric (soil water) potential of the soil. To illustrate this technique, data from the newly installed 229-L probe at the Norman Mesonet (NORM) site were examined. Typical ΔT values at NORM range from 1.3° (wet ground) to 3.4°C (dry ground) (Fig. 3; J. Basara 1997, personal communication).

Twenty measurements were made with each of the 221 available 229-L probes in both dry and saturated soils, and the average ΔT values were compiled. The average of all 4420 measurements was then used as the reference response. The range of sensor responses for a prescribed soil wetness can be greater than 1°C. Subsequently, adjustments were made to normalize each of the sensor responses. Then, individual sensors were tested against known values of soil water potential (ψ) in order to establish the relationship between sensor response and potential. The soil water potential is the work required to extract water from the soil against surface tension and is expressed as a negative value and in terms of work per mass of water. This value then can be multiplied by the density of water ($\sim$1000 kg m^{-3}) and be expressed as a pressure. Larger absolute values imply drier soil, because it takes more work to extract the remaining water. Statistical analysis of the sensor responses produced the following equation (Basara and Crawford 2000):

$$\psi = \frac{1}{a}\left[\left(\frac{dT_w - dT_d}{dT_{\text{ref}} - dT_d}\right) - 0.9\right]^{1/n}, \qquad (1)$$

where

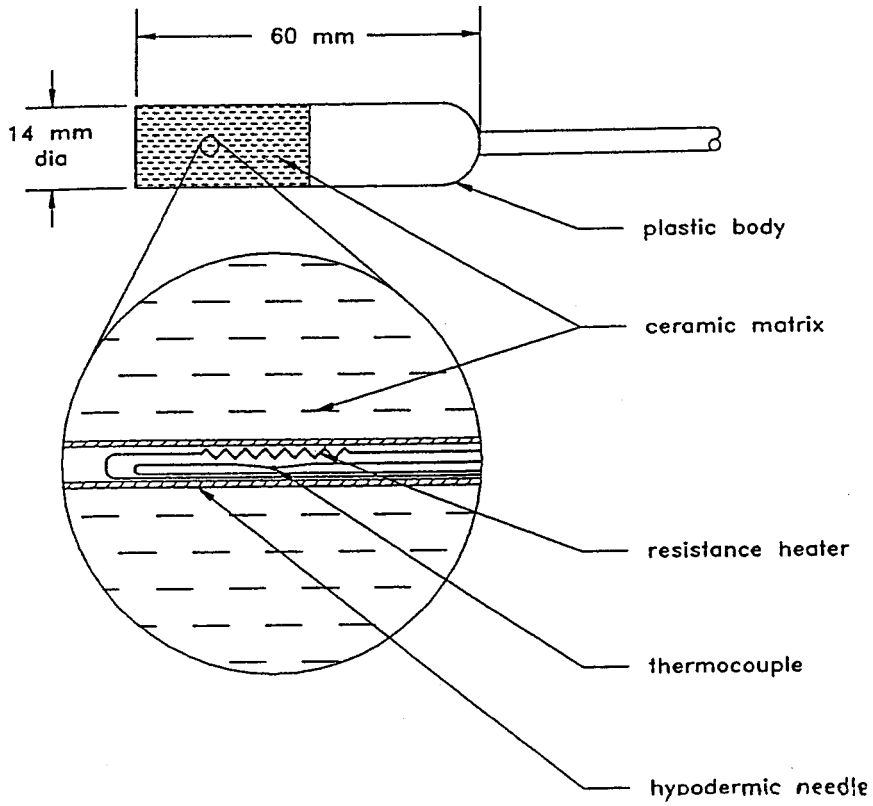

FIG. 2. Schematic of the CSI 229-L matric potential sensor.

$$a = -0.01 \text{ kPa}^{-1}, \qquad dT_w = 1.45^\circ\text{C},$$

$$dT_d = 4.0^\circ\text{C}, \qquad n = 0.77, \quad \text{and}$$

$$dT_{\text{ref}} = b_1 \Delta T + b_2, \tag{2}$$

where b_1 and b_2 are two calibration coefficients that are unique to each sensor.

The volumetric water content η describes the ratio of water volume to soil volume in a given soil column. Values theoretically can range from 0 to 1, but they generally remain below 0.5. To calculate η, a calibration equation relating η to ψ was employed (Basara and Crawford 2000):

$$\eta = \eta_r + \frac{\eta_s - \eta_r}{\{1 + [\alpha(-\psi/100)]^n\}^{(1-1/n)}}, \tag{3}$$

where η_r and η_s are the residual and saturated water content, and α and n are empirical calibration constants. Each soil moisture sensor has unique values of η_r, η_s, α, and n that are representative of the soil surrounding the sensor at a given site. Values of η_r (η_s) range from 0.0 to 0.2 (0.40–0.51). Calculated values of η were compared with more accurate gravimetric measurements at 17 selected sites in Oklahoma and Kansas over a 2-week period and were found to be accurate to ± 0.05. Note that there can be significant horizontal variations in η over a very small area (Famiglietti et al. 1999), and that these point measurements may not always be representative of the site, however (J. Schneider 1998, personal communication). Also, there is some evidence that the calibration constants may be sensitive to soil temperature.

A qualitative check of the soil moisture data at the 60 sites during July 1997 revealed an interesting problem. At 22 of the sites, just after a rainfall and when the topsoil was relatively dry, the increase in soil moisture was observed at 60 and 75 cm, with no apparent signal at 5 and 25 cm. It is hypothesized that the water was flowing along the instrumentation wire to the lower levels and was bypassing the upper levels. This curious problem deserves further study (Basara and Crawford 2000), but for our purposes, data from these stations will not be used.

The meteorological data used to drive SHM were provided by the Oklahoma Climatological Survey (OCS). Data from Mesonet daily summaries (1 January–31 July) were used as input to the model. These summaries were composed of maximum, minimum, and average values of air temperature (1.5 m), relative humidity (1.5 m), and wind speed (10 m); total rainfall, rain duration, and maximum rain rate; and total solar flux integrated over the day. The details of SHM are now described.

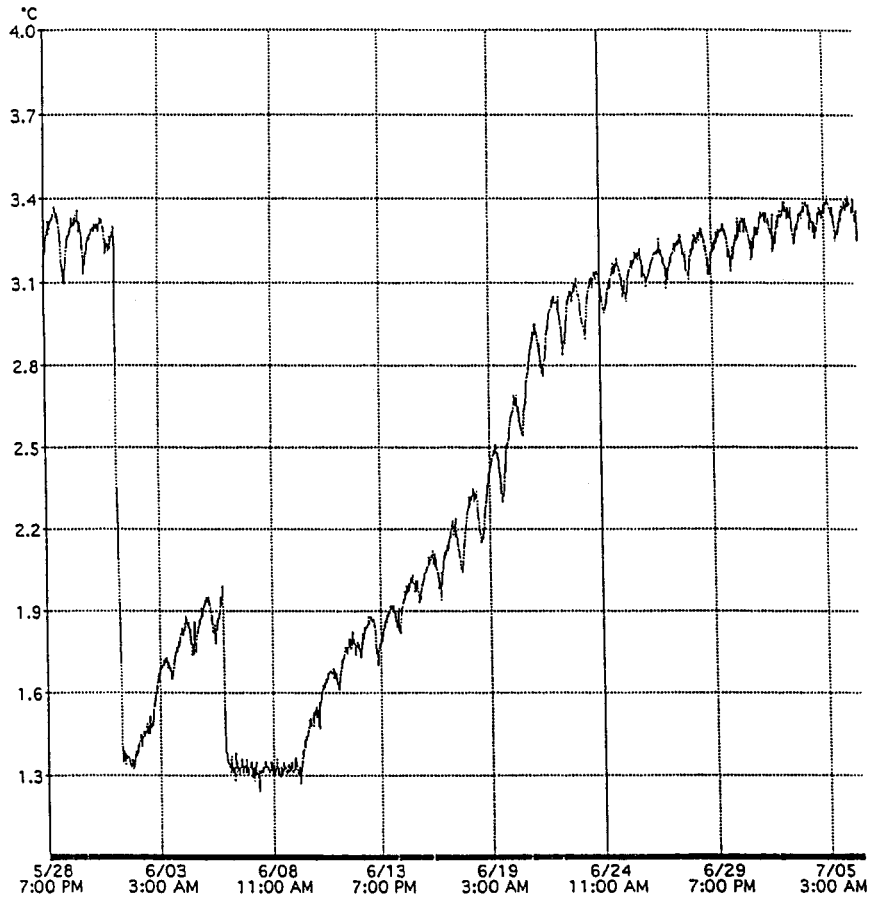

FIG. 3. Response of the 229-L probe (ΔT) at the NORM Mesonet site at a depth of 5 cm from 28 May to 5 Jul 1996. The diurnal oscillation likely is due to vertical transport of soil moisture during the day from evapotranspiration.

3. Model

For this study, the vertical water profile was calculated by SHM at an interval of 5 cm to a depth of 1 m. Precipitation infiltration provides the water input to the model, evapotranspiration (ET) provides the moisture extraction, and diffusion and gravitation act to transfer the water vertically within the soil. A daily precipitation value was input to the model every 24 h, and ET was calculated every 24 h. The diffusion (using Crank–Nicholson) and gravitation (using forward-in-time, backward-in-space) terms were calculated every 12 h. The atmospheric forcing occurs at 24-h intervals: average cloud cover was calculated by taking the ratio of the total daily solar input and total daily clear-sky solar input and subtracting the value from 1.0, and the daily dewpoint temperature was assumed to be the minimum air temperature. SHM was designed to use standard daily meteorological data, so that it can be run across a large area without the need for special high-resolution observations.

The precipitation input is allowed either to infiltrate into the soil or to be intercepted by the vegetation. An infiltration depth of 10 cm was used at all locations and all times in SHM, because sensitivity studies (not shown) showed that this depth yields the best results. The rainwater is distributed over the infiltration layer using a conic weighting function that varies from a maximum at the surface to zero at the infiltration depth. If the rain rate exceeds 1.3 cm h^{-1}, then 0.2 cm of water is allowed to accumulate on the vegetation. For smaller rates, 0.1 cm is intercepted. This water subsequently is allowed to evaporate when atmospheric conditions allow. Model values of η were bounded between η_r and η_s, whose values were determined uniquely at each Mesonet location.

Vegetation rooting depth was set to 0.8 m at all locations. This depth was chosen because an inspection of the 75-cm soil moisture data revealed consistent decreases during the month at all but one of the Mesonet sites, implying that the vegetation was able to tap soil water at this depth during this time. Vegetation height was specified to vary linearly with longitude, from 0.1 m in the extreme western

Panhandle to 1.0 m along the eastern Oklahoma border. This simple assumption was necessary because there are no real-time observations of vegetation height available at the sites. Soil types at each site have been determined through field surveys by OCS but also could be determined using the 1-km State Soil Geographic (U.S. Department of Agriculture 1994) soil type database for the contiguous United States. The dominant soil type at each location was prescribed at all soil depths. Model values of soil water potential and hydraulic conductivity at saturation are dependent on soil type and were taken from Cosby et al. (1984), along with an empirical coefficient b used to calculate the soil water potential and hydraulic conductivity.

The ET was calculated using the Penman–Monteith equation (Penman 1948; Monteith 1965) for both bare soil and vegetation, where

$$\mathrm{ET} = \frac{M}{\gamma + \Delta M}\left[(R_n - G)\Delta + \frac{\rho c_p (e_s - e)}{r_a}\right], \quad (4)$$

where γ is the psychrometric constant, Δ is the change in saturation vapor pressure e_s with respect to air temperature T at T, e is the observed vapor pressure, M is the moisture availability (described below), R_n is the net radiation, G is the ground heat flux, ρ is the air density, c_p is the specific heat capacity at constant pressure, and r_a is the atmospheric resistance to evaporation.

The moisture availability for the vegetation canopy is defined as

$$M_v = \frac{r_a}{r_a + r_s}, \quad (5)$$

where r_a is

$$r_a = \frac{C}{uk^2}\left[\ln\left(\frac{z_w}{z_0}\right)\right]^2. \quad (6)$$

Here, C is an atmospheric stability coefficient, which quantifies the effects of buoyancy on vertical fluxes of momentum, heat, and moisture. For this study, C was set to 0.85 (after Capehart and Carlson 1994) to represent the bulk reduction of aerodynamic resistance during the day. No ET was allowed at night, because the evaporation that may occur on the windiest and wettest nights is likely to be offset by dewfall on clear, calm nights. The measured wind speed at 10 m is represented by u, k is the von Kármán constant (0.4), z_w is the height of the wind measurement (10 m), and z_0 is the roughness length [one-eighth the vegetation height or 0.001 m for bare soil (Garratt 1992)].

The surface resistance r_s is a quantitative measure of the willingness of the vegetation to allow transpiration to occur. Small (large) values represent healthy (dormant) vegetation and relatively high (low) rates of transpiration. Previous studies (Jarvis 1976; Federer 1979; Noilhan and Planton 1989) have shown that the magnitude of r_s is related to the solar radiation, vapor pressure deficit, air temperature, and soil moisture. Avissar and Pielke (1991) also stressed the importance of ''leaf age,'' or elapsed time in the growing season. Because initial tests with the original formulation of r_s in SHM indicated that ET was much too small, relationships between r_s and these five factors were established in Oklahoma using linear regression and observations from the Atmospheric and Radiation Measurements (ARM) Program (Stokes and Schwartz 1994). Here, r_s is defined empirically as a sum of resistances (Crawford and Bluestein 2000):

$$r_s = \sum_{i=1}^{5} r_{si}, \quad (7)$$

where

$$r_{s1} = (e_s - e)/20, \quad (8)$$

$$r_{s2} = \begin{cases} 85 - 0.1(\mathrm{SW}_d) & \text{if } (e_s - e) \geq 500 \text{ Pa} \\ 0 & \text{if } (e_s - e) < 500 \text{ Pa} \end{cases} \quad (9)$$

(where SW_d is the measured incoming solar radiation),

$$r_{s3} = \begin{cases} -10(T - 30) & \text{if } T \geq 30^\circ\mathrm{C} \\ 0 & \text{if } T < 30^\circ\mathrm{C} \end{cases} \quad (10)$$

(where T is the measured air temperature at 1.5 m),

$$r_{s4} = \begin{cases} -2(\psi + 330)/5 & \text{if } \psi \leq -330 \text{ kPa} \\ 0 & \text{if } \psi > -330 \text{ kPa}, \end{cases} \quad \text{and} \quad (11)$$

$$r_{s5} = \begin{cases} \{80 - 115 \sin[\pi(\mathrm{day} - 110)/170]\} & \text{if longitude} \geq -97^\circ \quad \text{and} \quad 110 < \mathrm{day} < 270 \\ 80 & \text{if longitude} \geq -97^\circ \quad \text{and} \quad \mathrm{day} < 110 \quad \text{or} \quad \mathrm{day} > 270 \\ 0 & \text{if longitude} < -97^\circ \end{cases} \quad (12)$$

(where day is the yearday).

Comparisons with retrieved values of r_s from the ARM central facility in Lamont, Oklahoma, revealed a mean bias error of 5.9 s m^{-1} and a root-mean-square error of 30.0 s m^{-1}, or approximately 30% of a typical value.

The new r_s parameterization accounts for 95% of the variance of the retrieved values and leads to improved calculations of ET in the model.

The vapor pressure deficit dependence r_{s1} describes how the vegetation stomata close to conserve water during dry conditions. The solar radiation dependence r_{s2} describes how stomata open with increasing sunlight so that photosynthesis can occur. The r_{s3} dependence illustrates the opening of stomata in very warm temperatures as a means of regulating the surface temperature of the vegetation via transpirative cooling. When the soil is very dry, the stomata close to conserve water, as illustrated by the r_{s4} term. Last, r_{s5} describes a sinusoidal variation associated with leaf age during the growing season in eastern Oklahoma. Here, resistance is minimized during the middle part of the growing season and maximized at the beginning and end, when the vegetation is more sensitive. A similar variation was not found in western Oklahoma (longitude $< -97°$), presumably because of different vegetation types.

The moisture availability for the bare soil follows (Deardorff 1978):

$$M_s = \frac{\eta - \eta_r}{\eta_s - \eta_r}. \tag{13}$$

The magnitude of transpiration is conically weighted throughout the root zone; the evaporation from the bare soil is conically weighted throughout the top 10 cm. Net radiation is calculated using the average cloud cover and simple parameterizations for albedo, surface, and atmospheric emissivity, and downwelling longwave radiation. The ground heat flux G is parameterized as $0.1R_n$.

The fractional vegetation cover (FVC) for each of the 38 sites was calculated from a map of maximum normalized difference vegetation index (during the period 4–17 July 1997) using a formulation from Gutman and Ignatov (1998). Because the model simulation began on 1 January, FVC initially was set to zero and then was allowed to increase sinusoidally through spring and summer to the maximum value specified by the July FVC map. Total ET is a combination of the evaporation from the bare soil and the transpiration from the native vegetation (using the associated values of M and r_a for each process) at a given location, weighted by the fractional coverage of each.

The soil water profile was initialized by specifying 35% of the saturated volumetric water content at all levels. According to Capehart and Carlson (1994), the modeled soil water profile in the top 40 cm becomes independent of the assumed initial soil water profile 2–6 months into the simulation, given a sufficient number of wetting and drying cycles. Once the model is ''balanced,'' it is driven almost completely by ambient environmental conditions. To ensure that the model would be balanced by July, it was initialized on 1 January.

Vertical transfer of water is handled by Richards's equation, which describes Darcy flow:

$$-\frac{\partial q}{\partial z} = \frac{\partial}{\partial z}\left(K\frac{\partial \psi}{\partial \eta}\frac{\partial \eta}{\partial z}\right) + \frac{\partial K}{\partial \eta}\frac{\partial \eta}{\partial z}, \tag{14}$$

where q is the vertical moisture flux, and K is the hydraulic conductivity. The first term on the right-hand side of the equation represents diffusion and the second represents gravitation. The Clapp and Hornberger (1978), van Genuchten (1980), and Cosby et al. (1984) formulations for K and ψ were all tested, with little difference in the model output. The Cosby et al. (1984) formulation was used in this study because of its slightly better performance. Equation (14), along with a calculation of the source and sink terms, provides for the total change in water content in a time step at a given location:

$$\frac{\partial \eta}{\partial t} = -\frac{\partial q}{\partial z} + \text{infiltration} - \text{ET}. \tag{15}$$

4. Comparisons with observations

The daily Mesonet soil moisture observations from 2330 UTC were compared with the SHM daily output from July 1997 at 38 Mesonet sites at 5, 25, 60, and 75 cm. Daily averages (over all 38 sites) of both observations and model output were computed at all four soil levels (Fig. 4). At 5 cm (Fig. 4a), the model estimates η to within $\sim$0.03 m m^{-3} (the observational error is 0.05), and, more important, the *changes* in η are modeled very well. The 25-cm comparisons (Fig. 4b) depict similar behavior during the first half of the month. On yearday 198, there is a significant rise in observed η that was accompanied by a less significant rise in the model. The subsequent observed drying, beginning at yearday 200, does not appear in the model for four more days. Last, the small increase in observed η at day 209 also is unresolved by the model, possibly because of the lag exhibited in the model response.

At 60 cm (Fig. 4c), the sluggishness of the model response is even more apparent, and the model error is approaching the size of the observational uncertainty. Both observations and model output depict the climatological midsummer deep-soil drying regime throughout the month, and the slope of the model response is very close to that of the observed drying trend. Although the heavy rain event that caused the sharp observed response at 5 and 25 cm on day 198 is also apparent at 60 cm, the model response is very weak, with only a slight change in output noted. The comparisons at 75 cm (Fig. 4d) depict similar behavior.

The behavior of the data at the three lower soil levels on day 198 is notable, because there was no similar response to the widespread rain events on days 184 and 190 (as manifested by sharp changes in 5-cm soil moisture in Fig. 4a). In soil with high clay content such as that found in Oklahoma, changes in η are accompanied by significant changes in porosity. This shrinking (drying) and swelling (wetting) eventually will result in

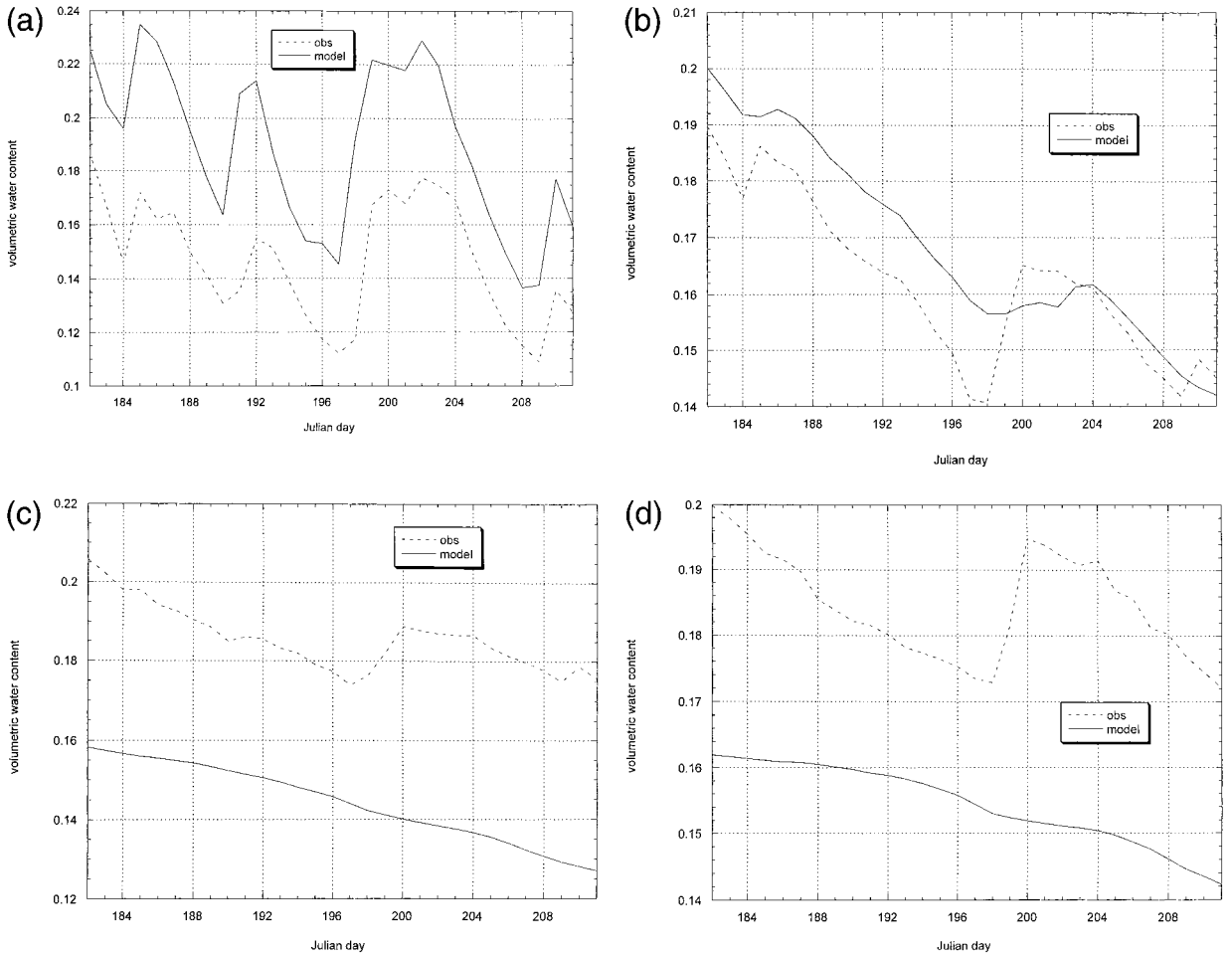

FIG. 4. Comparisons of the daily 38-station average of η between SHM and Mesonet observations during Jul 1997 at (a) 5, (b) 25, (c) 60, and (d) 75 cm.

cracked soil. These cracks then provide preferential pathways for water to flow deeper into the clay soils (Marshall et al. 1996). This process may explain the increase in η at 25, 60, and 75 cm during the day-198 rainfall event, because there were two cycles of wetting and drying earlier in the month.

A more objective analysis was performed at each depth by combining the data from all the sites for the entire month into scatterplots. At 5 cm (Fig. 5a), it is apparent that the model slightly overestimates η, as depicted by the orientation of the best-fit regression line with respect to the ''perfect-fit'' line. This result also confirms the comparison made in Fig. 4a. The root-mean-square error (rmse) of 0.09 represents approximately 20% of the observed range of values. At 25 cm (Fig. 5b), there is significantly more scatter in the data, and it is apparent that there is significant correlation between nearby groups of data points. These clusters represent data from a single site and depict month-long biases in the model output at that site. The character of the plots from 60 and 75 cm (Figs. 5c,d) are similar to each other, depicting reasonable agreement between the model and observations for η values below 0.2, but exhibiting significant model underestimation of η in wetter conditions. This lack of model response to rainfall events at lower levels at some of the sites is one of the causes of the clustering of data points in Figs. 5b–d.

To understand better the unusual nature of the comparisons at the deeper levels, two sites will be examined in more detail. At STIL (Fig. 6a; see Fig. 1 for location), the lowest three levels are saturated until day 191, when they finally begin to dry out, starting at 25 cm. A rainfall event of 77 cm on days 198–199 then effectively saturates the entire vertical profile. In the model (Fig. 6b), however, this significant rainfall has a very limited effect on the deeper soil moistures. Also, the modeled values of η at 60 and 75 cm are less than half of the observed values. One possible explanation for the exceedingly high observed values at STIL may be an anomalously high water table, which would act to keep the lower levels saturated even in the driest of summer months. Water-table height variations from site to site are not modeled at all but may play important roles in modulating deeper soil moistures at some sites.

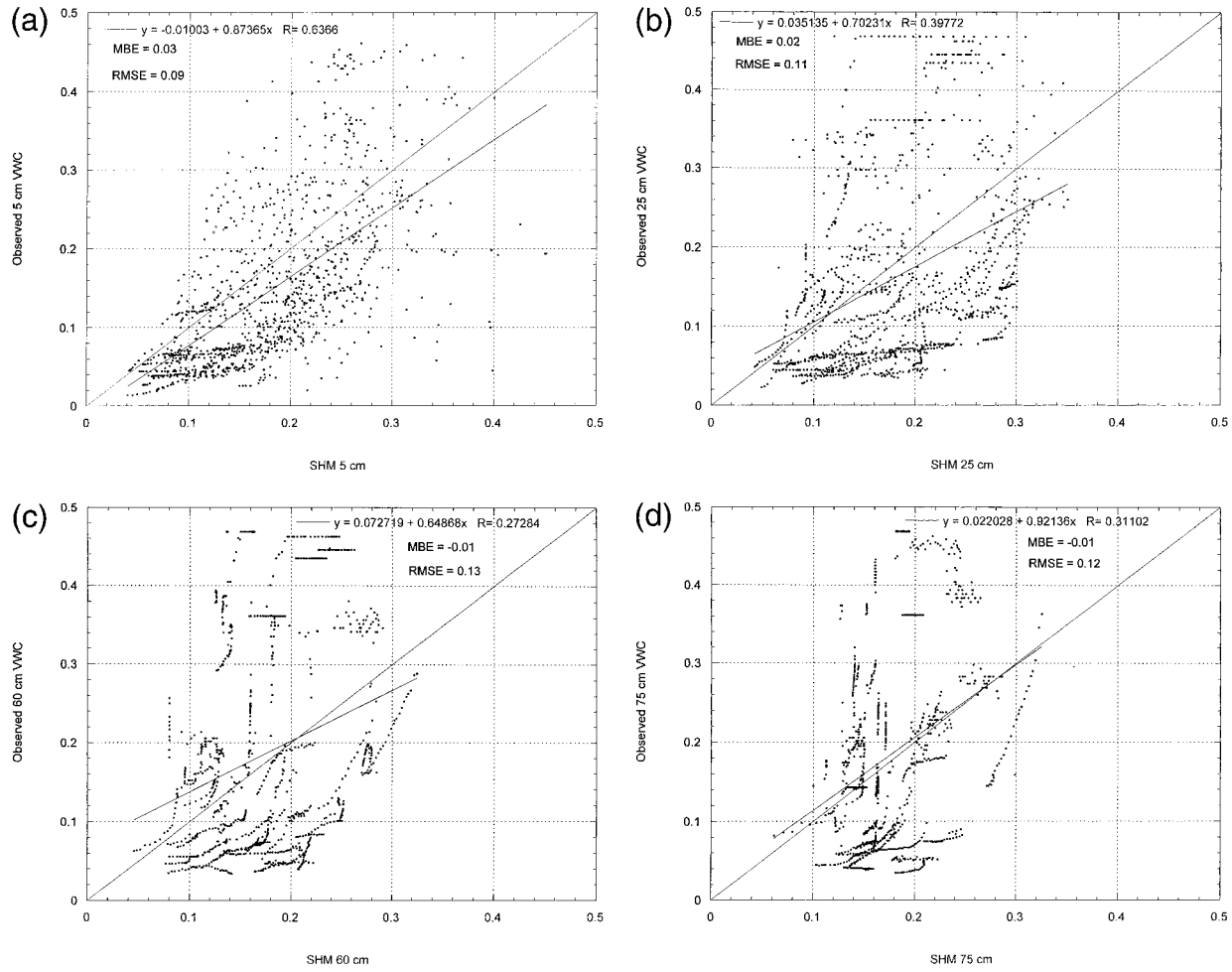

FIG. 5. Scatterplots comparing observed and modeled η values at all 38 Mesonet stations during Jul 1997 at (a) 5, (b) 25, (c) 60, and (d) 75 cm.

In contrast, at EUFA (Fig. 1 and Fig. 7a), the observations at 60 and 75 cm remained very dry throughout the month and were not affected by the rainfall events on days 184, 201–202, and 209. The model results (Fig. 7b) were qualitatively similar, with the only significant changes in η found at 5 and 25 cm. The magnitudes of the model variations are muted in comparison with the observations, however. Also, the relatively steady modeled values of η at the two deeper layers were significantly higher than the observations. It is possible that certain sites like EUFA may have anomalously large vegetation rooting depths, allowing more soil water to be extracted from the deeper layers.

An examination of similar observations from other sites has accentuated further this striking lack of consistency from site to site across the domain. Therefore, it should not be surprising that SHM exhibits significant errors at the deeper soil levels at many of the sites. Until we can understand better the highly localized variation in the character of the deep-layer soil moisture profiles found in nature, it is doubtful that any hydrological model will perform well when compared with point observations of η. The results do suggest, however, that SHM may be used to calculate an accurate regionally averaged value of η (see Fig. 4), which then can be used (rather than predicting unique values for each grid box) to initialize deep-layer soil moisture in numerical prediction models.

A crude model analysis of the total amount of water in the 1-m soil column can be done by simply looking at the mean bias errors (MBEs) for the different levels. On average, the model was slightly too wet at 5 and 25 cm and slightly too dry at 60 and 75 cm. The average MBE over the four depths, 0.01, implies that the total amount of water in the soil column was being modeled well and that the model errors are due mainly to problems in reproducing the correct vertical transfer of water within the soil.

5. Conclusions

SHM has been modified, and daily predictions of soil water content were made at 38 Oklahoma Mesonet sites

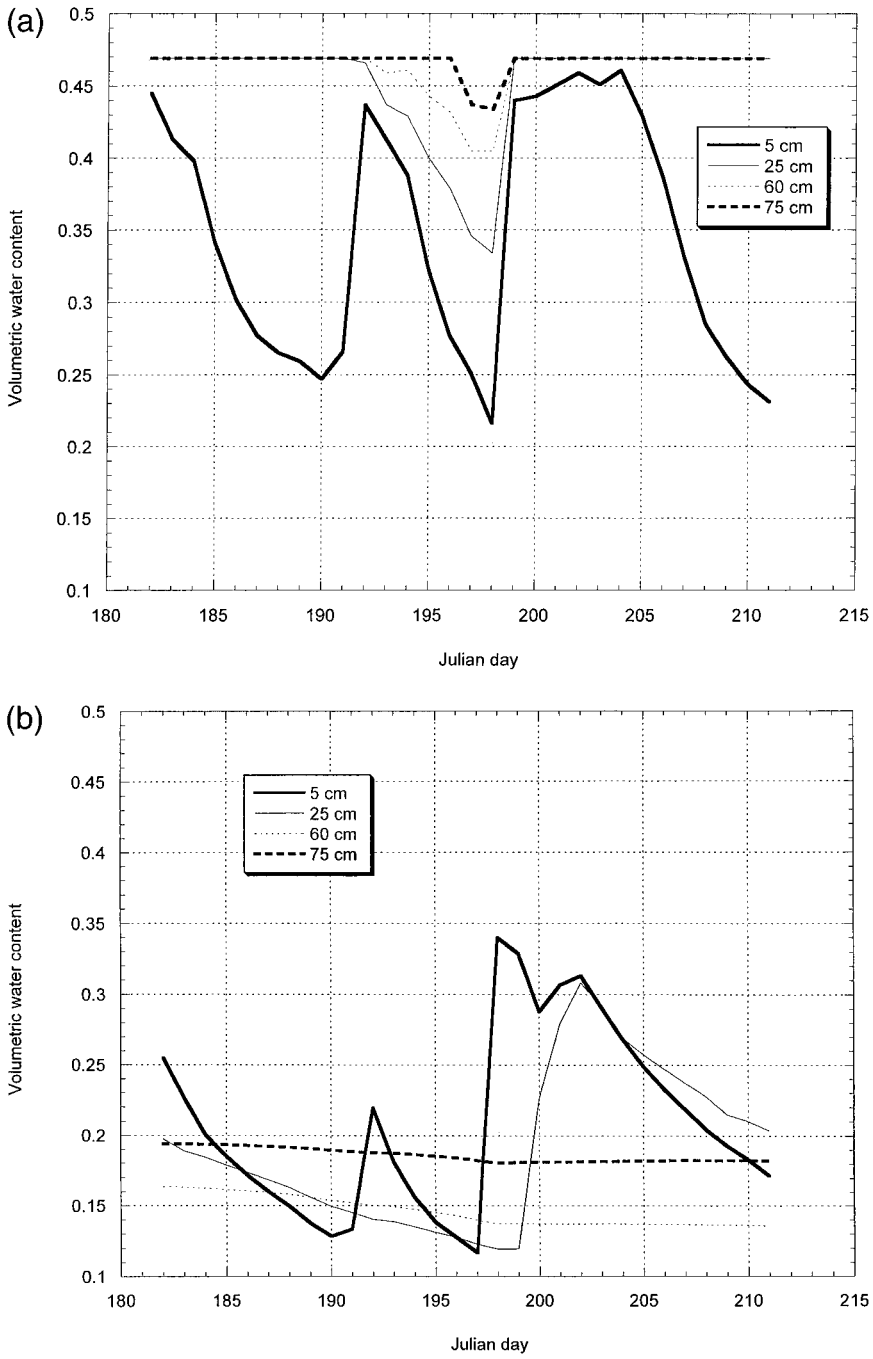

FIG. 6. (a) Observed and (b) modeled daily values of η at STIL at all four levels during Jul 1997.

during July 1997. Using daily climate summaries as input, the model was able to predict accurately the changes in soil moisture at 5 cm, exhibiting a slight wet bias within the range of observational uncertainty. The comparisons at 25, 60, and 75 cm were also characterized by small biases, but the model response to changes in soil moisture was more sluggish with increasing depth. The model biases at all levels were within observational error. It was hypothesized that cracks in the soil, which may have formed from repeated episodes of wetting and drying, may be responsible for some of the rapid increases in observed soil water at the lower levels. If true, this fact would explain part of the sluggish model response, because this process is not currently modeled by SHM (or other soil models).

The verification of a hydrological model with in situ

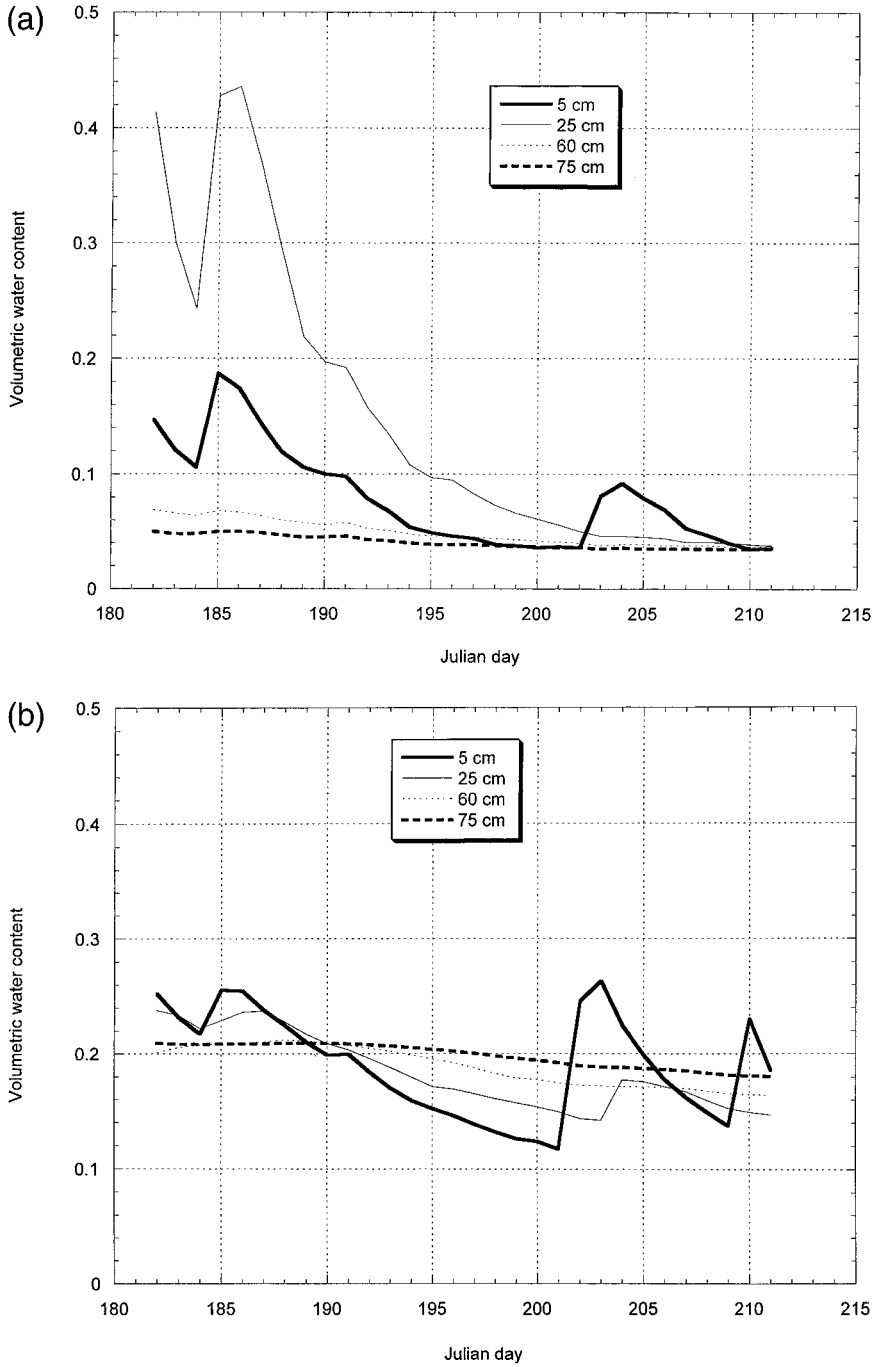

FIG. 7. Same as Fig. 6, but for EUFA.

observations over such a broad area ($\sim 10^5$ km^2) and at such high spatial resolution ($\sim$50 km) is believed to be unique. The promising results from this work suggest that the feasibility of using SHM to initialize soil moisture in numerical models should be investigated further. Estimates of soil type, fractional vegetation cover, precipitation, average cloud cover, minimum air temperature, and vegetation height would be required at each model grid box to produce reasonable predictions of η. These data requirements can be achieved through a judicious combination of standard meteorological observations, output from numerical models, and satellite-derived products. Our results suggest that point values of η at 5 cm can be modeled reasonably well by SHM; for deeper soil levels, only the regionally averaged value can be reproduced accurately. The use of regionally av-

eraged values for validation at deeper levels effectively accounts for sharp variations in soil properties that may render point observations unrepresentative. Future improvements in the model should focus on representing the cycles of contracting and swelling of clay soils, along with a more precise specification of the change in soil texture with depth.

Acknowledgments. This study was funded by NSF Grant EPS-9871807. We thank Mercedes Lakhtakia for providing the original SHM code and documentation. Two anonymous reviews, along with a review by Jeanne Schneider, greatly improved the manuscript.

REFERENCES

Avissar, R., and R. A. Pielke, 1991: The impact of plant stomatal control on mesoscale atmospheric circulations. *Agric. For. Meteor.*, **54,** 353–372.

Basara, J. B., and T. M. Crawford, 2000: Improved installation procedures for deep-layer soil moisture measurements. *J. Atmos. Oceanic Technol.,* **17,** 879–884.

Black, T. L., 1994: The new NMC Mesoscale Eta Model: Description and forecast examples. *Wea. Forecasting,* **9,** 265–278.

Brock, F. V., K. C. Crawford, R. L. Elliott, G. W. Cuperus, S. J. Stadler, H. L. Johnson, and M. D. Eilts, 1995: The Oklahoma Mesonet: A technical overview. *J. Atmos. Oceanic Technol.,* **12,** 5–19.

Capehart, W. J., and T. N. Carlson, 1994: Estimating near-surface soil moisture availability using a meteorologically driven soil-water profile model. *J. Hydrol.,* **160,** 1–20.

——, and ——, 1997: Decoupling of surface and near-surface soil water content: A remote sensing perspective. *Water Resour. Res.,* **33,** 1383–1395.

Cherkauer, K. A., and D. P. Lettenmaier, 1999: Hydrologic effects of frozen soils in the upper Mississippi River basin. *J. Geophys. Res.,* **104,** 19 599–19 610.

Clapp, R. B., and G. M. Hornberger, 1978: Empirical equations for some soil hydraulic properties. *Water Resour. Res.,* **14,** 601–604.

Cosby, B. J., G. M. Hornberger, R. B. Clapp, and T. R. Ginn, 1984: A statistical exploration of the relationships of soil moisture characteristics to the physical properties of soils. *Water Resour. Res.,* **20,** 682–690.

Crawford, T. M., and H. B. Bluestein, 2000: An operational, diagnostic surface energy budget model. *J. Appl. Meteor.,* **39,** 1196–1217.

Deardorff, J. W., 1978: Efficient prediction of ground surface temperature and moisture, with inclusion of a layer of vegetation. *J. Geophys. Res.,* **83,** 1889–1903.

Dudhia, J., 1993: A nonhydrostatic version of the Penn State–NCAR Mesoscale Model: Validation tests and simulation of an Atlantic cyclone and cold front. *Mon. Wea. Rev.,* **121,** 1493–1513.

Famiglietti, J. S., and Coauthors, 1999: Ground-based investigation of spatial–temporal soil moisture variability within remote sensing footprints during SGP97. *Water Resour. Res.,* **35,** 1839–1851.

Federer, C. A., 1979: A soil–plant–atmosphere model for transpiration and availability of soil water. *Water Resour. Res.,* **15,** 555–562.

Garratt, J. R., 1992: *The Atmospheric Boundary Layer*. Cambridge University Press, 316 pp.

Groves, J. R., 1989: A practical soil moisture profile model. *Water Resour. Bull.,* **25,** 875–880.

Gutman, G., and A. Ignatov, 1998: Derivation of green vegetation fraction from NOAA/AVHRR for use in numerical weather prediction models. *Int. J. Remote Sens.,* **19,** 1533–1538.

Jarvis, P. G., 1976: The control of transpiration and photosynthesis by stomatal conductance found in canopies in the field. *Philos. Trans. Roy. Soc. London,* **273B,** 593–610.

Liang, X., D. P. Lettenmaier, E. F. Wood, and S. J. Burges, 1994: A simple hydrologically based model of land surface water and energy fluxes for GSMs. *J. Geophys. Res.,* **99,** 14 415–14 428.

——, E. F. Wood, and D. P. Lettenmaier, 1996: Surface soil parameterization of the VIC-2L model: Evaluation and modification. *Global Planet. Change,* **13,** 195–206.

Mahfouf, J. F., 1991: Analysis of soil moisture from near-surface parameters: A feasibility study. *J. Appl. Meteor.,* **30,** 1534–1547.

Marshall, T. J., J. W. Holmes, and C. W. Rose, 1996: *Soil Physics*. Cambridge University Press, 453 pp.

Monteith, J. L., 1965: Evaporation and environment. *Proc. 19th Symposium of the Society for Experimental Biology,* Soc. Exp. Biol., 205–235.

Noilhan, J., and S. Planton, 1989: A simple parameterization of land surface processes for meteorological models. *Mon. Wea. Rev.,* **117,** 536–549.

Penman, H. L., 1948: Natural evaporation rates from open water, bare soil and grass. *Proc. Roy. Soc. London,* **A194,** 120–145.

Pereira Fo., A. J., and K. C. Crawford, 1999: Mesoscale precipitation fields. Part I: Statistical analysis and hydrologic response. *J. Appl. Meteor.*, **38,** 82–101.

Reece, C. F., 1996: Evaluation of a line heat dissipation sensor for measuring soil matric potential. *Soil Sci. Soc. Amer. J.,* **60,** 1022–1028.

Smith, C. B., M. N. Lakhtakia, W. J. Capehart, and T. N. Carlson, 1994: Initialization of soil-water content in regional-scale atmospheric prediction models. *Bull. Amer. Meteor. Soc.*, **75,** 585–593.

Stokes, G. M., and S. E. Schwartz, 1994: The Atmospheric Radiation Measurement (ARM) Program: Programmatic background and design of the Cloud and Radiation Test Bed. *Bull. Amer. Meteor. Soc.,* **75,** 1201–1221.

U.S. Department of Agriculture, 1994: State Soil Geographic (STATSGO) data base. Data use information. Miscellaneous Publication 1492, 33 pp. [Available from National Cartography and GIS Center, U.S. Department of Agriculture, Soil Conservation Sevice, P.O. Box 6567, Fort Worth, TX 76115-6567.]

van Genuchten, M. T., 1980: A closed-form equation for predicting the hydraulic conductivity of unsaturated soils. *Soil Sci. Soc. Amer. J.*, **44,** 892–898.

Vieux, B. E., and N. Gauer, 1994: Finite-element modeling of storm water runoff using GRASS GIS. *Microcomput. Civil Eng.*, **9,** 263–270.

Wetzel, P. J., and J.-T. Chang, 1988: Evapotranspiration from nonuniform surfaces: A first approach for short-term numerical weather prediction. *Mon. Wea. Rev.,* **116,** 600–621.